

## Influence of $\text{KMnO}_4$ Substitution on the Structural and Transport Properties of $\text{Tl}_2\text{Ba}_2\text{Ca}(\text{Cu}_{1-x}\text{R}_x)_2\text{O}_{\delta+6}$ System

Belqees Hassan,<sup>1\*</sup> Ali Alnakhilani,<sup>1</sup> Abdulhafiz Muhammad<sup>2</sup>  
and Muhammad Ali Al-Hajji<sup>3</sup>

<sup>1</sup>Faculty of Sciences, Department of Physics, Ibb University, Ibb, Yemen

<sup>2</sup>Faculty of Sciences, Department of Physics, Damascus University, Syria

<sup>3</sup>Faculty of Civil Engineering, Department of Basic Science, Damascus University, Syria

\*Corresponding author: belqees.ahmad@yahoo.com

Published online: 25 November 2016

To cite this article: Hassan, B. et al. (2016). Influence of  $\text{KMnO}_4$  Substitution on the Structural and Transport Properties of  $\text{Tl}_2\text{Ba}_2\text{Ca}(\text{Cu}_{1-x}\text{R}_x)_2\text{O}_{\delta+6}$  System. *J. Phys. Sci.*, 27(3), 13–24, <http://dx.doi.org/10.21315/jps2016.27.3.2>

To link to this article: <http://dx.doi.org/10.21315/jps2016.27.3.2>

**ABSTRACT:** *The effect of partial replacement of  $R = \text{KMnO}_4$  in  $\text{Tl}_2\text{Ba}_2\text{Ca}(\text{Cu}_{1-x}\text{R}_x)_2\text{O}_{\delta+6}$  (TBCCO or Tl-2212) superconductor samples with  $x = 0.0, 0.05$  and  $0.1$  was investigated. The samples were prepared by standard solid-state reaction methods in a sealed quartz tube under normal pressure. The investigation consisted of X-ray diffraction (XRD) and DC electrical resistance measurements under fixed magnetic field. Transport measurements indicated that the superconducting transition temperature values of the samples depend on the amount of the added  $\text{KMnO}_4$ . The values of  $T_c$  and  $T_o$  of the samples decreased with increasing  $\text{KMnO}_4$  content. The possible reasons for the observed degradation in the superconducting and microstructure properties of Tl-2212 due to the addition of  $\text{KMnO}_4$  were discussed.*

**Keywords:** Partial replacement, solid state reaction, electrical resistance, transition temperature, microstructure

### 1. INTRODUCTION

Since the discovery of the high-temperature ceramic superconductors, numerous studies have been carried out to characterise the properties of these materials.<sup>1–8</sup> The optimum hole concentration in the conducting  $\text{CuO}_2$  planes is the source of the highest critical temperature in the high  $T_c$   $\text{Tl}_2\text{Ba}_2\text{Ca}(\text{Cu}_{1-x}\text{R}_x)_2\text{O}_{\delta+6}$  (Tl-2212) superconductor.

Doping with various elements was found to be useful and effective for enhancing the high-temperature superconductivity (HTS) properties.<sup>1</sup> In an earlier work, the effect of  $\text{KMnO}_4$  doping on the properties of Tl-based superconductors was studied.<sup>10</sup> We found the optimum amount of  $\text{KMnO}_4$  at which the properties of the Tl-based superconductor are improved. Here, we analyse the structure and study the electrical properties of the  $\text{KMnO}_4$ -doped Tl-based superconductor synthesised at the optimum conditions. Characterisation of the temperature and magnetic field dependencies of HTS is of considerable importance for both theoretical and applied fields of science.

The  $\text{CuO}_2$  planes play a crucial role in the  $\text{HT}_c$  TBCCO superconducting family. The effect of the substitution on the Cu sites has the much stronger effect than that on the other sites because substitutions/dopings directly affect the superconductivity owing to the changes in  $\text{CuO}_2$  plane properties. A superconductor-insulator transition (SIT) can occur owing to the impurities that increase the scattering of the carriers in the  $\text{CuO}_2$  planes and/or owing to the variations of the carrier concentration by substitutions in the material.<sup>11</sup>

The intercalation of oxygen ( $\text{O}_\delta$ ) in the charge reservoir layer controls the flow of carriers toward the conducting  $\text{CuO}_2$  planes, i.e., an optimum amount of  $\text{O}_\delta$  would help the electrons to flow toward the conducting  $\text{CuO}_2$  planes.<sup>12</sup>

The replacement process has an important effect on two parameters. First, the replacement process increases or decreases the oxygen content in the sample. If there is a decrease in the oxygen content, we observe a tail in the R-T curve of the samples. Mezzetti et al.<sup>13</sup> found that the Y-123 system exhibits a pronounced tail in the low temperature region of the R-T curve, likely due to the off-stoichiometric oxygen content. On the other hand, when the replacement process increases the oxygen content, there is an increase in the pressure inside the quartz tube, which is the second parameter that is strongly affected by the replacement process. The increased pressure inside the quartz tube allows the formation of other phases inside the sample.

In the TBCCO system, the suppression of  $T_c$  due to the substitution/doping of other elements on Cu sites has been attributed to the Abrikosov and Gor'kov pair-breaking mechanism.<sup>14,15</sup> Variation of the carrier concentration (particularly holes) in the  $\text{CuO}_2$  planes, unbinding of the Cooper pairs and carrier localisation induced by the structural disorder are also useful for explaining the decrease in  $T_c$ .<sup>16</sup>

In this study, we have prepared superconducting samples of  $\text{Tl}_2\text{Ba}_2\text{Ca}(\text{Cu}_{1-x}\text{R}_x)_2\text{O}_{\delta+6}$ , where  $\text{R} = \text{KMnO}_4$ , and  $x = 0.5, 1.0$  and  $2.0$  using a solid-state reaction

technique. Microstructure, electrical, and magnetic properties of these samples were investigated.

## 2. EXPERIMENTAL

Samples with the nominal composition of  $\text{Tl}_2\text{Ba}_2\text{CaCu}_2\text{O}_{6+\delta}$  (TBCCO) were synthesised by the conventional single-step solid-state reaction technique. Stoichiometric amounts of highly pure  $\text{Tl}_2\text{O}_3$ ,  $\text{BaO}_2$ ,  $\text{CaO}$  and  $\text{CuO}$  were mixed using an agate mortar to make fine powder that was sieved in  $64\ \mu\text{m}$  sieves to obtain a homogeneous mixture. The powder was pressed in the form of a disc with the diameter and thickness of 1.5 cm and 0.2 cm, respectively. Then, the samples were wrapped in a silver foil to reduce the thallium evaporation during the preparation. To protect the furnace from possible hazardous effects, a sealed quartz tube with a diameter of 1.5 cm and length of 15 cm was placed in a closed stainless steel protecting tube. Finally, the sealed tube was placed horizontally in a furnace, heated at the rate of  $4^\circ\text{C}\ \text{min}^{-1}$  to  $820^\circ\text{C}$ , and held at this temperature for 4 h, followed by cooling to room temperature at the rate of  $0.5^\circ\text{C}\ \text{min}^{-1}$ . To obtain the optimally doped Tl-2223 superconducting material, the samples were annealed in normal atmosphere at  $500^\circ\text{C}$ .

The electrical resistivity of the prepared samples was measured by the conventional four-probe technique from room temperature down to the zero resistivity temperature using a closed cryogenic refrigeration system employing helium gas as the working medium.

The samples have the shape of parallel sides with the approximate dimensions of  $15 \times 2 \times 3\ \text{mm}^3$ ; the connections of the copper leads with the sample were made using a conductive silver paint, and a constant current of 2 mA provided from a Keithley 2400 current source is passed through the sample during resistance measurements in the four-probe method in order to avoid the heating of the samples.

We use a Keithley 2400 Source Meter as the DC bias source because it can be operated in either the voltage or current source mode. In all experiments, the stable magnetic field up to 12 T was applied by a Lake Shore Superconducting Magnet System and the temperature of the sample was controlled precisely within 1 mK. During the cooling process, both the Keithley Source Meter and Lakeshore temperature controller are controlled by the LabVIEW software.

### 3. RESULTS AND DISCUSSION

#### 3.1 Powder X-ray Diffraction Analyses

Figure 1 shows the X-ray diffraction scans of  $\text{Tl}_2\text{Ba}_2\text{Ca}(\text{Cu}_{1-x}\text{R}_x)_2\text{O}_{\delta+6}$ , superconductor samples ( $\text{R} = \text{KMnO}_4$ ,  $x = 0.0$  and  $0.1$ ). The pattern peaks for  $x = 0$ , and  $0.1$  can be indexed using the P4/mmm space group of the Tl-2212 phase with a tetragonal unit cell, and small traces of the Tl-1212 phase and unknown peaks.

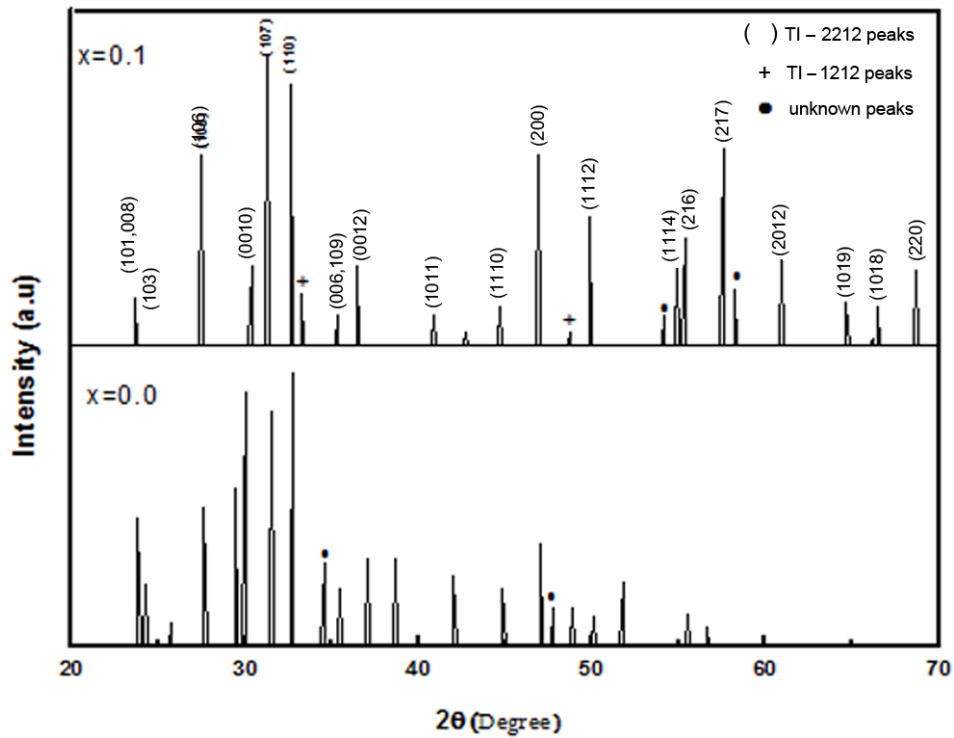


Figure 1: Powder XRD patterns for  $\text{Tl}_2\text{Ba}_2\text{Ca}(\text{Cu}_{1-x}\text{R}_x)_2\text{O}_{\delta+6}$ , superconductor samples with  $\text{R} = \text{KMnO}_4$ , ( $x = 0.0$  and  $0.1$ ).

The crystal symmetry of the sample is tetragonal and the unit cell parameters of the sample (i.e.,  $a$  and  $c$ ) were found to be  $a = 3.8355^\circ\text{A}$  and  $c = 29.6081\text{A}^\circ$ , close to the typical values of the Tl-2212 phase.<sup>16</sup>

The lattice parameters " $a$ " and " $c$ " as functions of  $\text{KMnO}_4$  content are listed in Table 1. Examination of the data in the table clearly shows that the changes in the lattice parameters " $a$ " and " $c$ " are insignificant. The calculated lattice parameters

of the Tl2212 phase showed an increase of both the a- and c-lattice parameters with the  $\text{KMnO}_4$  content. It is possible that substitution of smaller  $\text{Mn}^{7+}$  (ionic radius 0.25 Å) for the larger  $\text{CuO}_{2+}$  spacer ion (ionic radius 0.73 Å) caused the increase in the "a" and "c"-lattice parameters.

Table 1:  $T_{c \text{ onset}}$ ,  $T_{c \text{ zero}}$ , room-temperature resistance at 300K and lattice parameters of  $\text{Tl}_2\text{Ba}_2\text{Ca}(\text{Cu}_{1-x}\text{R}_x)_2\text{O}_{\delta+6}$

Samples	$T_{c \text{ onset}}$ (K)	$T_{c \text{ zero}}$ (K)	Resistance at 300K( $\Omega$ )	a=b (Å°)	c (Å°)
x = 0	113	97	0.478	3.8355	29.6081
x = 0.05	108	20	2.896	–	–
x = 0.1	112	58	2.681	3.8427	29.6211

### 3.2 Electrical Resistance (DC) Measurements

The curves for the normalised resistance versus temperature of  $\text{Tl}_2\text{Ba}_2\text{Ca}(\text{Cu}_{1-x}\text{R}_x)_2\text{O}_{\delta+6}$ , ( $\text{R} = \text{KMnO}_4$ ,  $x = 0.0, 0.05$  and  $0.1$ ) are shown in Figure 2. The  $x = 0.0$  sample exhibits a sharp superconducting transition. In agreement with the XRD spectra, this sharp phase transition indicates that the sample is a single phase Tl-2212. The  $x = 0.05$  sample has a second phase and reaches the zero resistance value smoothly when the temperature reaches 20K. On the other hand, the  $x = 0.1$  sample shows a sharp transition, and its resistance reaches zero at 58K. Comparing this sample with the  $x = 0.05$  sample shown in Figure 2, we note that the second phase and the long tail found in  $x = 0.05$  sample have disappeared in the  $x = 0.1$  sample. This may be related to the added  $\text{KMnO}_4$  absorbing the excessive oxygen and acting as a controller of the pressure. This means that this sample has been improved. For the 0.0 and 0.1 samples, the variation of the resistance with the temperature is found to be linear from room temperature to 125K. A linear variation of the normal-state resistance reveals that the electron-phonon scattering is the dominant mechanism down to the  $T_c$  of each sample. For the  $x = 0.05$   $\text{KMnO}_4$ -substituted sample, a small resistance drop was obtained at 108K. This suggests that this sample consists of a mixed phase of  $\text{HT}_c$  superconducting materials. Substitution of  $\text{KMnO}_4$  at the Cu site of this sample led to a change from the metallic behaviour and a decrease in the  $T_c$  and  $T_0$  values of the samples.

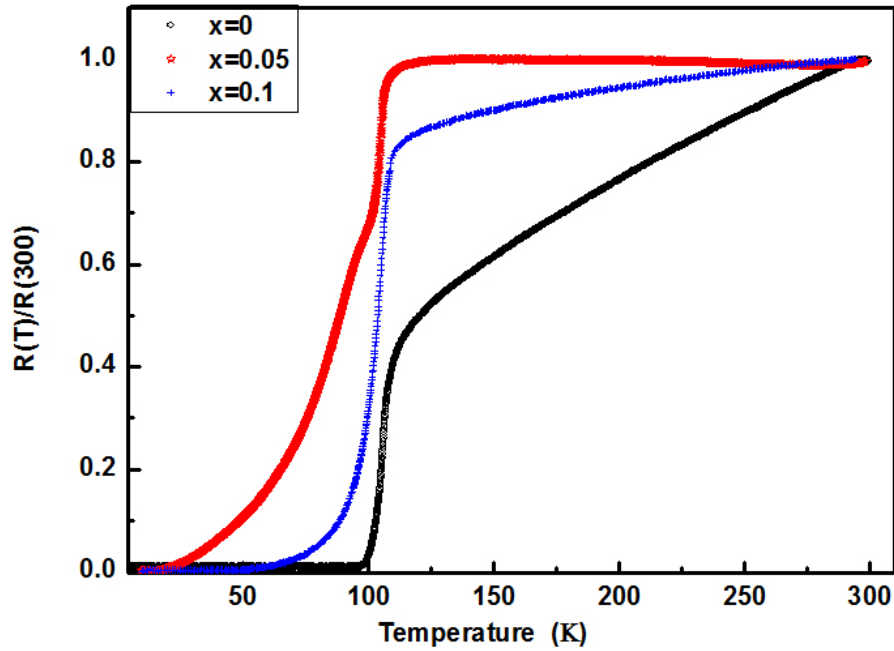


Figure 2: Temperature dependence of normalised resistance for the samples.

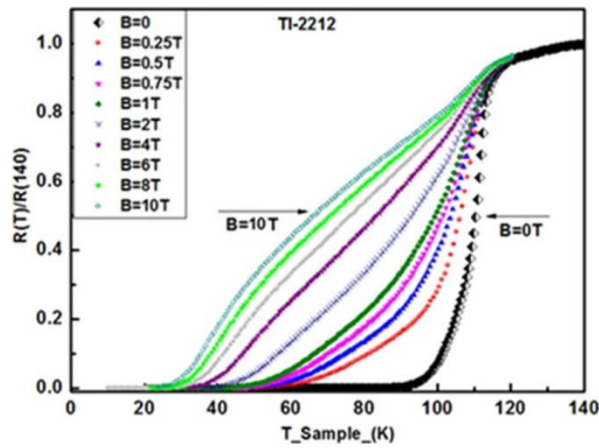
Table 1 shows the values of  $T_c$  onset,  $T_c$  zero, resistivity (at 300 K), and Tl2212 lattice parameters for  $\text{Tl}_2\text{Ba}_2\text{Ca}(\text{Cu}_{1-x}\text{R}_x)_2\text{O}_{\delta+6}$ , ( $\text{R} = \text{KMnO}_4$ ,  $x = 0.0, 0.05$  and  $0.1$ ). The room temperature resistance in these samples varies from  $0.478$  to  $2.681 \Omega$ . These samples showed the onset of superconductivity ( $T_c^{\text{onset}}$ ) at approximately 113K, 108K and 112K and zero resistance critical temperatures  $\{T_c(\text{R} = 0)\}$  of approximately 97, 20 and 58K for  $x = 0.0, 0.05$ , and  $0.1$ , respectively. Initially,  $T_c(\text{R} = 0)$  decreases with added  $\text{KMnO}_4$  and then starts to increase.

As shown in Figure 2,  $\text{KMnO}_4$ -added samples showed a broad transition, indicating the presence of impurities and weak links between the superconducting grains. The increase of the transition width and appearance of double-step behaviour indicate that the  $\text{KMnO}_4$ -added samples have a greater number of grain boundaries because the double-step resistive transition is an indication of weak links.<sup>17,18</sup>

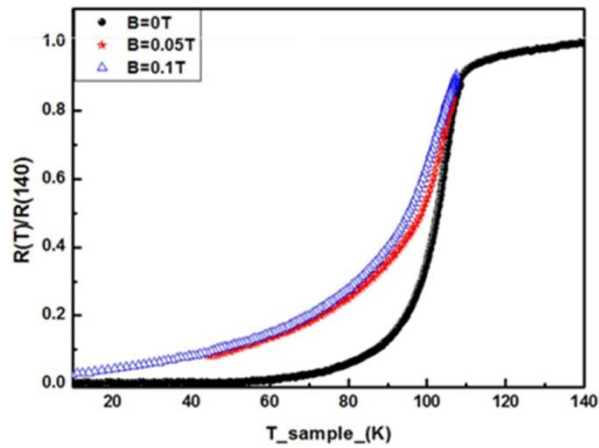
It is well-known that substitutions on the Cu sites have a very strong effect on the superconducting properties. In particular, the electronic configuration of the system is destroyed by the substitution of  $\text{KMnO}_4$  for  $\text{Cu}^{2+}$ , causing the reduction of the electronic conductivity in the CuO planes through the formation of impurity bonds. Therefore, the superconducting phase coherence is destroyed.

### 3.3 Effect of DC Magnetic Field Results

To investigate the effect of  $\text{KMnO}_4$  substitution on the superconducting properties of the samples, we performed DC magnetic field measurements. We only measured the effect of the DC magnetic field up to 10 T of the  $x = 0.0$  sample because the other samples ( $x = 0.05, 0.1$ ) did not show superconducting properties below 77K. The magnetoresistance versus temperature curves of the  $x = 0.0$  and 0.1 samples under different magnetic fields are shown in Figures 3(a–b) as an example. The applied magnetic field strongly affect the superconducting transition temperature  $T_c$ .



(a)



(b)

Figure 3:  $R$ - $T$  curves under different magnetic field up to 10 T for the samples with (a)  $x = 0.0$ , (b)  $x = 0.1$

All samples show a metallic behaviour in the high temperature region followed by a superconducting transition as the temperature was lowered. The superconducting transition width ( $\Delta T_c$ ), which is the difference between the superconducting transition temperature ( $T_{c, \text{onset}}$ ) and the zero resistance temperature ( $T_{\text{zero}}$ ) ( $\Delta T_c = T_{c, \text{onset}} - T_{\text{zero}}$ ) was analysed in two different stages. The main steep part of the resistance remains almost unchanged by the application of magnetic field. In the first stage, at just below the onset of the transition temperature very close to  $T_{c, \text{onset}}$ , the structure can be associated with the intergrain transitions; thus, an applied field of up to 10 T does not appreciably affect the intragranular transition. This is also related to the absence of the flux traps because vortex pinning is ineffective in this first stage as previously noted by many groups.<sup>19</sup> The broadening effect induced by the applied magnetic fields is similar to that in the  $\text{HT}_c$  systems.

However, the tail was enlarged significantly in the second stage. We believe that the pinning of vortices is highly effective and therefore, the resistance depends strongly on the applied magnetic field. Therefore, the change of the resistance (tails in the second stage) is due to the thermally activated flux creep process. However, in the  $x = 0.1$  sample, no  $T_0$  value was obtained under the applied magnetic field of 1 T. We believe that intergrowth of the impurity phases in the main matrix and weak coupling formation between the grains play an important role in decreasing of the superconductivity.

As shown in Figure 3(a, b), the tail region represents the interactions of the grain boundaries at which the magnetic field easily destroys the interactions between the grains while the superconductivity inside the grains is preserved. Similar results were obtained by other research groups.<sup>20-23</sup>

The temperature dependence of the calculated upper critical field ( $H_{c2}$ ) values for the Tl-2212 sample is plotted in Figure 4. It was found that  $H_{c2}(T)$  values increased with decreasing temperature.  $H_{c2}(0)$  was calculated from the extrapolation of the sample  $H_{c2}(T)$  to  $T = 0\text{K}$ .<sup>24,25</sup> The  $H_{c2}(0)$  value was 22.3 T, corresponding to the 10% of the value of the resistivity measured in the normal state  $\rho_n(T)$  at 140K.

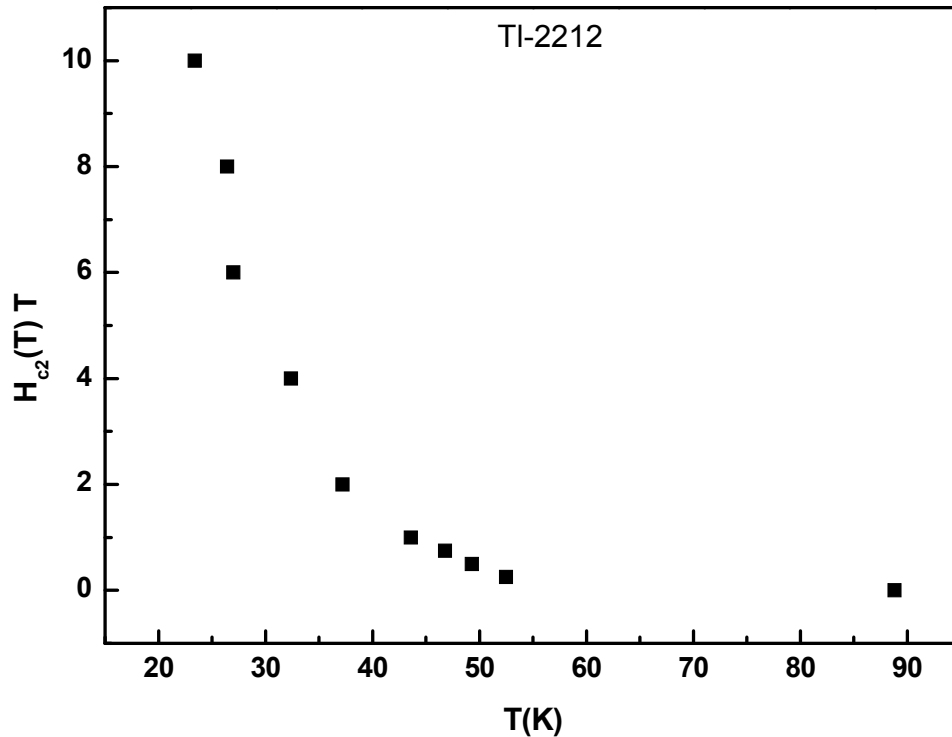


Figure 4: Upper critical magnetic field  $H_{c2}(T)$  vs.  $T_c$  for the x = 0 sample.

#### 4. CONCLUSION

In the present work, the effects of  $\text{KMnO}_4$  substitution on the phase evolution and transport properties of the TBCCO (TI-2212) system were studied. It is believed that the incorporation of the  $\text{KMnO}_4$  particles into the interstitial sites in the material rather than the occupation of the Cu sites caused a change in the unit cell parameters.  $T_c$  and  $T_0$  decreased monotonically as a result of the substitution of  $\text{KMnO}_4$  into the TI-2212 system. The weak coupling between the  $\text{KMnO}_4$  particles and TBCCO grains and the decrease of the carrier concentration were found to affect  $T_c$  and  $T_0$ . The analyses of crystal structures are important for understanding the properties of high- $T_c$  superconductors and for exploring new materials. The upper critical magnetic field  $H_{c2}(0)$  at  $T = 0\text{K}$  for 10% of  $R_n$  was calculated by the extrapolation of  $H_{c2}(T)$  to  $T = 0\text{K}$ .

## 5. ACKNOWLEDGMENT

The authors would like to thank Damascus University in Syria for providing facilities and support to setup the testbed. This original research was proudly supported by the Ibb University in Yemen.

## 6. REFERENCES

1. Duan, H., et al. (1991). Anisotropic resistivity and paraconductivity of  $\text{Tl}_2\text{Ba}_2\text{CaCu}_2\text{O}_8$  single crystals. *Phys. Rev. B*, 43(16), 12925–12929, <http://dx.doi.org/10.1103/PhysRevB.43.12925>.
2. Kim, D., Gray, K. & Trochet, M. (1992). Scaling behavior of fluctuation conductivity of high-temperature superconductors in a magnetic field. *Phys. Rev. B*, 45(18), 10801–10804, <http://dx.doi.org/10.1103/PhysRevB.45.10801>.
3. Abou-Aly, A. et al. (2001). Effect of cooling rate and strontium doping on the formation of (Hg, Tl)-1234 phase. *Supercond. Sci. Technol.*, 14(8), 637–642.
4. Sundaresan, A. et al. (2003). Preparation of Tl-2212 and Tl-1223 superconductor thin films and their microwave surface resistance. *IEEE Trans. Appl. Supercon.*, 13(2), 2913-2916, <http://dx.doi.org/10.1109/TASC.2003.812045>.
5. Huda, N. & Yahya, A. K. (2009). Effects of Cu substitution on superconductivity and excess conductivity of  $\text{Tl}_{1-x}\text{Cu}_x\text{Sr}_{1.8}\text{Yb}_{0.2}\text{CaCu}_2\text{O}_{7-\delta}$  ( $x=0-0.6$ ) ceramics. *Mater. Res. Innovat.*, 13(3), 406–408, <http://dx.doi.org/10.1179/143307509X441685>.
6. Ahmad, N. H., Khan, N. A. & Yahya, A. (2010). Superconducting fluctuation behavior and infrared absorption properties of  $\text{Tl}_{1-x}\text{Cu}_x\text{Sr}_{1.6}\text{Yb}_{0.4}\text{CaCu}_2\text{O}_{7-\delta}$  and  $\text{Tl}_{0.5}\text{Pb}_{0.5}\text{Sr}_{2-y}\text{Mg}_y\text{Ca}_{0.8}\text{Yb}_{0.2}\text{Cu}_2\text{O}_{7-\delta}$  ceramics. *J. Alloys Comp.*, 492(1), 473–481, <http://dx.doi.org/10.1016%2Fj.jallcom.2009.11.144>
7. Abou-Aly, A. et al. (2009). Excess conductivity analysis for  $\text{Tl}_{0.8}\text{Hg}_{0.2}\text{Ba}_2\text{Ca}_2\text{Cu}_3\text{O}_{9-\delta}$  substituted by Sm and Yb. *Solid State Com.*, 149(7), 281–285, <http://dx.doi.org/10.1016%2Fj.ssc.2008.12.003>.
8. Ali Yusuf, A. et al. (2011). Effect of  $\text{Ge}^{4+}$  and  $\text{Mg}^{2+}$  doping on superconductivity, fluctuation induced conductivity and interplanar coupling of  $\text{TlSr}_2\text{CaCu}_2\text{O}_{7-\delta}$  superconductors. *Phys. C Supercon.*, 471, 363–372, <http://dx.doi.org/10.1016/j.physc.2011.03.007>.
9. Hassan, B., Abdulhafiz, M. & Hajji, M. A. A. (2013). Effect of thallium doping on the electrical and magnetic properties of  $(\text{Hg}_x\text{Tl}_{1-x})_2\text{Ba}_2\text{CaCu}_2\text{O}_{\delta+6}$  superconductor phase. *Damascus Uni. J. Fundamen. Sci.*, 29(1), 105–118.

10. Hassan, B., Abdulhafiz, M. & Hajji, M. A. A. (2012). Effect of partial replacement of CuO by  $\text{KMnO}_4$  on superconducting properties in the (Hg,Tl)-2223 phase. *Damascus Uni. J. Fundamen. Sci.*, 28(2), 147–161.
11. Martynova, O. & Gasumyants, V. (2008). On the transformation of the normal-state band spectrum of Tl-based HTSC's with increasing number of  $\text{CuO}_2$  layers and doping level. *Phys. C Supercon.*, 468(5), 394–400, <http://dx.doi.org/10.1016/j.physc.2007.12.007>.
12. Khan, N. A. et al. (2013). Atmospheric pressure synthesis of Be- and Mg-doped  $\text{TlBa}_2\text{Ca}_2\text{Cu}_3\text{O}_{10-\delta}$  superconductor. *Ceramics Int.*, 39(2), 1901–1908.
13. Mezzetti, E. et al. (1999). Control of the critical current density in  $\text{YBa}_2\text{Cu}_3\text{O}_{7-\delta}$  films by means of intergrain and intragrain correlated defects. *Phys. Rev. B*, 60(10), 7623, <http://dx.doi.org/10.1103/PhysRevB.60.7623>.
14. Li, Q. et al. (2003). Substitution effect of Sn for Cu in the  $\text{Bi}_2\text{Sr}_2\text{CaCu}_{2-x}\text{Sn}_x\text{O}_{8+\delta}$  system. *J. Supercon.*, 13(1), 137–139, <http://dx.doi.org/10.1023/A:1007794613891>.
15. Aksan, M. A. & Yakinci, M. E. (2004). Synthesis and characterization of Er-substituted Bi-2223 H- $T_c$  glass-ceramic superconductors. *J. Alloys Comp.*, 385(1), 33–43, <http://dx.doi.org/10.1016/j.jallcom.2004.04.135>.
16. Kayed, T. & A. Qasrawi. (2005). Temperature and magnetic field effects on the carrier density and Hall mobility of boron-doped Tl–Ba–Ca–Cu–O superconductor. *J. Alloys Comp.*, 402(1), 5–11, <http://dx.doi.org/10.1016/j.jallcom.2005.04.148>.
17. Ozturk, O. et al. (2007). Substitution of Sm at Ca site in  $\text{Bi}_{1.6}\text{Pb}_{0.4}\text{Sr}_2\text{Ca}_{2-x}\text{Sm}_x\text{Cu}_3\text{O}_y$  superconductors. *Phys. B Condens. Mat.*, 399(2), 94–100.
18. Aliabadi, A., Farshchi, Y. A. & Akhavan, M. (2009). A new Y-based HTSC with  $T_c$  above 100K. *Phys. C Supercon.*, 469(22), 2012–2014, <http://dx.doi.org/10.1016/j.physc.2009.09.003>.
19. Aksan, M., Yakinci, M. & Güldeste, A. (2006). Co-addition into  $\text{MgB}_2$ : The structural and electronic properties of  $(\text{MgB}_2)_{2-x}\text{Co}_x$ . *J. Alloys Comp.*, 424(1), 33–40, <http://dx.doi.org/10.1016/j.jallcom.2005.12.066>.
20. Khosroabadi, H., Daadmehr, V. & Akhavan, M. (2003). Magnetic transport properties and Hall effect in  $\text{Gd}_{1-x}\text{Pr}_x\text{Ba}_2\text{Cu}_3\text{O}_{7-\delta}$  system. *Phys. C Supercon.*, 384(1), 169–177, [http://dx.doi.org/10.1016/S0921-4534\(02\)01876-2](http://dx.doi.org/10.1016/S0921-4534(02)01876-2).
21. Kameli, P. et al. (2008). Thermally activated flux creep in the  $\text{Bi}_{1.66}\text{Pb}_{0.34}\text{Sr}_2\text{Ca}_{2-x}\text{Mg}_x\text{Cu}_3\text{O}_y$  superconductors. *Phys. C Supercon.*, 468(3), 137–141.
22. Çelik, Ş. et al. (2008). Investigation of the dependency of the upper critical magnetic field on the content x in  $\text{Y}_{1-x}\text{Yb}_{x/2}\text{Gd}_{x/2}\text{Ba}_2\text{Cu}_3\text{O}_{7-y}$  superconducting structures. *J. Alloys Comp.*, 460(1), 79–82, <http://dx.doi.org/10.1016/j.jallcom.2007.06.037>.

23. Hassan, B., et al. (2015). A new method for determining the lower and upper critical magnetic field in Tl-2234 superconductor. *Aus. J. Basic Appl. Sci.*, 9(2), 34–39.
24. M. Erdem., et al. (2011). Effect of Gd addition on the activation energies of Bi-2223 superconductor. *Phys. B Condens. Matt*, 406,705–709, <http://dx.doi.org/10.1016/j.physb.2010.12.008>.
25. Sharma, D. et al. (2013). DC and AC susceptibility study of sol-gel synthesized  $\text{Bi}_2\text{Sr}_2\text{CaCu}_2\text{O}_{8+\delta}$  superconductor. *Ceramics Int.*, 39, 1143–1152.